Photodegradation of Polypropylene Containing a Nucleating Agent

M. S. RABELLO,* J. R. WHITE

Materials Division, Department of MMME, University of Newcastle upon Tyne, Newcastle upon Tyne, NE1 7RU, United Kingdom

Received 6 August 1996; accepted 26 November 1996

ABSTRACT: The effect of including 0.5 wt % talc on the photodegradation behavior of polypropylene (PP) was investigated in injection-molded samples exposed to ultraviolet radiation (UV) in the laboratory for periods of up to 24 weeks. The structure of the talc-nucleated samples was characterized by X-ray diffraction and light microscopy and compared with that of nonnucleated PP, and the information was used to explain the differences in their photodegradation behavior. Measurements of the extent of chemical degradation were made by Fourier transform infrared spectroscopy (FTIR) and gel permeation chromatography (GPC), and they showed that there is no significant effect of a nucleating agent on the kinetics of photooxidation. PP bars containing a nucleating agent showed a larger reduction in mechanical properties with UV exposure and a partial recovery in properties after prolonged exposure was observed with both types of samples. An increase in crystallinity during UV exposure (chemicrystallization) was detected by X-ray diffraction and differential scanning calorimetry (DSC) and the dependence with exposure time was similar in nucleated and nonnucleated samples. DSC was also used to determine the melting behavior and transition temperatures of the specimens during exposure and after recrystallization from the melt. © 1997 John Wiley & Sons, Inc. J Appl Polym Sci **64:** 2505–2517, 1997

INTRODUCTION

One of the most common ways to modify a polymer structure and morphology is by the incorporation of nucleating agents.[1–5] Normally used in low concentrations (up to 1 wt %), these compounds increase the rate of crystal nucleation by acting as heterogeneous nuclei. It is well known that a preexisting foreign surface within the polymer melt greatly reduces the free energy for the formation of a critical nucleus[6] and, consequently, an increase in the rate of crystallization is observed.[7,8] In the case of isotactic polypropylene, the use of nucleating agents is particularly important owing to its low rate of crystallization. If the polymer crystallizes faster, the injection-molding cycle can be shortened, increasing the industrial productivity. A great number of substances have been found to act as heterogeneous nuclei in the crystallization of polypropylene (PP),[9] with talc being one of the most frequently used.[10–16] Binsbergen[9] stressed that good nucleating agents for polyolefins are generally crystalline and insoluble in the melt and contain rows of polar and nonpolar groups on the surface. To tailor the nucleant activity, surface treatments are sometimes carried out.[16–19] Reviews on the general theory and mechanisms of heterogeneous nucleation of PP were published by Binsbergen[20] and, more recently, by Galeski.[6]

Although nucleating agents are widely used by industry to improve properties and reduce processing times, very few investigations to establish

---

Correspondence to: J. R. White.

* *Permanent address:* Department of Materials Engineering, Federal University of Paraiba, Av. Aprigio Veloso 882, Campina Grande, PB, Brazil.

Contract grant sponsor: EPSRC.

the degradation resistance of the nucleator-added polymers have been reported. Nevertheless, this theme has attracted some attention in recent times and studies involving PP[21–26] and other polymers[27] have been presented. However, most of these reports dealt with the effects of γ-radiation degradation. In general, it was found that the presence of nucleating agents decreases the radiation stability of the polymer, because the radicals generated in the crystal boundaries (that are present in higher proportion in nucleated polymers) can move more easily to the amorphous regions where degradation is faster.[21,22] A number of investigations were developed concerning the photodegradation of polymer composites,[28–34] but no report was found in the literature dealing with the photodegradation behavior of PP containing talc as a nucleating agent, despite the increasing use of this combination in outdoor applications.

The presence of a nucleating agent may affect the kinetics of photodegradation of PP in a number of ways, including the catalyst effect of metal ions present as impurities on the particle surface and the change in oxygen diffusion caused by a different microstructure in the host polymer. Furthermore, it is known that the mechanical properties of photodegraded PP are closely related to its initial structure and morphology, and the relative changes in properties do not necessarily follow the same trend of the kinetics of degradation. Aspects like spherulite size and molecular orientation may play a major role in the mechanical properties.

The effect of the addition of 0.5 wt % talc on the photodegradation behavior of injection-molded PP is the subject of the current article which is part of a more comprehensive investigation into the effects of polymer structure and morphology on the photooxidation of PP.[35,36] Various aspects of photodegradation are discussed here, including the extent of chemical degradation, mechanical properties, and fracture and the effects of UV radiation on the polymer structure. The structure of the starting materials are also described since there is a considerable change in the microstructure with the addition of talc. The photodegradation of PP filled with large amounts of talc (20–40 wt %) was dealt with elsewhere.[32]

EXPERIMENTAL

Material and Sample Preparation

Injection-molded tensile bars were prepared with a general purpose commercial grade of isotactic PP (ICI GXE 35). The tensile bars (3.1 mm thick) were produced using a Butler-Smith 100/60 injection-molding machine operating with the following conditions: injection pressure 107 MPa; barrel temperature 200°C (all zones); nozzle temperature 200°C; and mold temperature 40°C. The flow of the melted material into the mold was through a tab gate (thickness 0.5 mm) located at one end of the cavity. The gate left a witness mark that allowed identification of the back/front of the molding. This identification was important in the exposure procedure since the structure of the material near the bar front face was different to that near the back face. A minimum of 30 samples was rejected at the beginning of the production run to ensure that equilibrium conditions had been established in the molding machine.

The specimens containing the nucleating agent were prepared by tumble mixing granules of GXE 35 with 0.5 wt % talc prior to injection molding. The talc used was supplied by Aldrich with a reported particle size of < 10 μm. Although it is known that injection molding alone does not provide an intensive mixing of the components, the use of an additional mixing technique (like extrusion or internal mixing) was avoided because it would change the concentration of chromophores within the matrix through thermal degradation[37] and, hence, alter the kinetics of photodegradation. The bars containing the nucleating agent were labeled as NPP, whereas the nonnucleated ones were labeled as PP. After molding, all samples were kept at room temperature for at least 3 weeks before UV exposure to minimize postmolding aging effects such as secondary crystallization.

The choice of injection-molded bars rather than thin films (normally used for studying the kinetics of degradation) was made because it has a much more practical appeal—most nucleated polymers are processed by injection molding. The degradation in this case is confined to the specimen surface and this controls the mechanical behavior and fracture in ways that cannot be predicted from the behavior of isolated thin firms, as will be discussed further later on. The structure and morphology of the two types of samples are different and this is another aspect that is considered here.

Ultraviolet Exposure

The ultraviolet exposure was conducted at 30 ± 1°C in a constant temperature room following

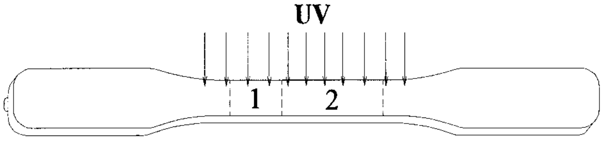

Figure 1 UV exposure arrangement. Section 1 was used for X-ray diffraction experiments, whereas section 2 was used for DSC, FTIR, and GPC measurements.

other studies in this laboratory.[31,35,38] The source of UV radiation was UVA–340 fluorescent tubes supplied by Q-Panel Co. The tubes (1.2 m long) were used in pairs, producing a uniform output over the central meter. The intensity reaching the sample was measured weekly using a Bentham spectroradiometer and set to 2.2 Wm^{-2} in the wavelength range 290–320 nm. The bars were exposed with the face opposite to the tab gate facing the UV source (Fig. 1). The penetration of UV radiation through the two types of specimens showed similar characteristics, with comparable values of absorption coefficients and reflectivities.[39]

Extent of Chemical Degradation

The extent of chemical degradation was measured by Fourier transform infrared spectroscopy (FTIR) and gel permeation chromatography (GPC). Samples used for the analyses were collected by gathering the material milled away to a depth of 0.2 mm from the exposed surface of the test bar. To avoid inconsistencies in sampling procedures, all analyses were done on specimens removed from section 2 of Figure 1.

Infrared spectra were obtained in transmission with a Nicolet 20 PC-IR Fourier transform spectrometer. The equipment was set to operate in the range 400–4000 cm^{-1} with a resolution of 4 cm^{-1}, obtaining a spectrum that represented the average of 32 scans. A carbonyl index was computed as the relative areas under the carbonyl peak (1700–1800 cm^{-1}) and a reference peak, not affected by photooxidation (centered at 2720 cm^{-1}).

GPC measurements were made at Rapra Technology Ltd. using a 300 mm-length column filled with gel supplied by Polymer Laboratories (PL gel 2 × mixed gel-B) with a particle size of 10 μm. Solutions with 1,2-dichlorobenzene were run at 140°C with a flow rate of 10^{-6} m^3/min and an injection volume of 0.2×10^{-6} m^3/min. Discussion on the procedure adopted by Rapra to measure the molecular weight of degraded polymers was presented elsewhere.[40]

Mechanical Behavior and Fractography

The injection-molded bars were tensile tested using a JJ Lloyd T5003 testing machine with a crosshead speed of 50 mm/min. The error bars shown in this study represent the standard deviation of four experiments. The fractured bars were retained for surface inspection which was conducted using a Hitachi S-2400 scanning electron microscope, after applying a gold coating to minimize charging problems.

Differential Scanning Calorimetry (DSC)

A Mettler FP90 controller connected to an FP85 heat flux DSC cell was used with specimens (weighing 5–6 mg) removed from the exposed surface by milling away a depth of 0.2 mm in section 2 of Figure 1. The equipment was calibrated for temperature and calorimetric sensitivities of the cell with indium. Thermograms were recorded under nitrogen flow (50×10^{-6} m^3/min) using a heating rate of 13°C/min, from 40 to 210°C. After melting, the specimens were recrystallized at a cooling rate of 13°C/min and, finally, a reheating scan was conducted with the same heating rate. The results reported here represent the average of three separate experiments.

Structural Characterization

X-ray diffraction measurements were carried out with a Phillips PW 1050 diffractometer using CuKα Ni-filtered radiation (wavelength = 0.154 nm) in the diffraction angle range $2\theta = 7–31°$. Since the polymer structure may vary with the distance from the injection-molded gate,[41,42] all X-ray diffraction analyses were conducted in specimens removed from section 1 of Figure 1. From the traces obtained, the fractional crystallinity (f_c) was calculated according to the method developed by Weidinger and Hermans.[43] According to the authors, this method gives results that are in agreement with those obtained by the method of Ruland[44] but without the rigor and time-consuming procedures of the latter. The crystal orientation distribution of the starting materials was determined by pole figure analysis using a Phillips PW 1078 instrument operating in reflection only (maximum tilting angle of 70°). The pole figures reported here were constructed with data obtained with the Bragg angle corresponding to the (040) planes of PP (at $2\theta = 16.9°$).

Polarized light microscopy observations were

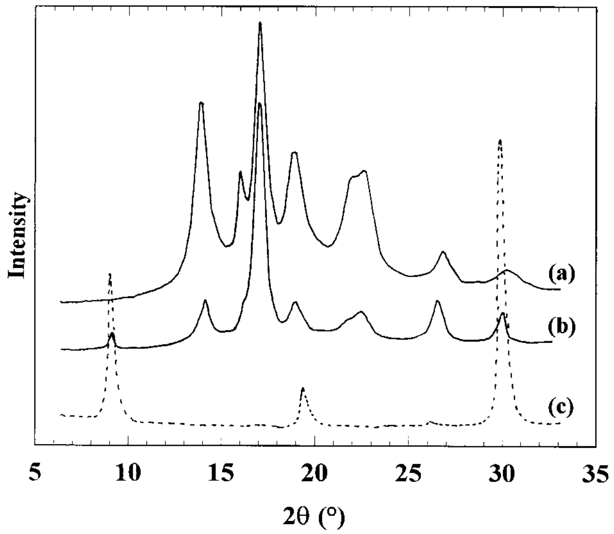

Figure 2 X-ray diffractograms of (a) nonnucleated PP, (b) nucleator-added PP (NPP), and (c) pure talc used as the nucleating agent.

conducted using an Olympus microscope (Model BH-2). Thin sections (10–20 μm) were microtomed perpendicular to the molding direction from the central part of the bars and mounted between two glass slides. Very sharp microtome knives were necessary to obtain slices free from scratches.

RESULTS AND DISCUSSION

Structure of the As-molded Materials

Figure 2 compares the X-ray diffractograms of PP containing the nucleator (NPP) and nonnucleated PP. There are some reflections due to the talc particles in the NPP diffractogram as is evident by comparing with the diffractogram of pure talc [Fig. 2(c)]. The main difference between the PP reflections for NPP and PP is a much stronger reflection from (040) planes in NPP samples. By conducing the diffraction measurement with the sample in other orientations (Fig. 3), it is shown that the PP crystals in NPP have a strong orientation with the *b*-axis lying perpendicular to the molding direction (i.e., in the normal direction [ND], Fig. 3). The preferred orientation of the *b*-axis was confirmed by pole figure analysis (Fig. 4). This figure also shows that the *b*-axis orientation in PP is stronger in the material containing talc. The high orientation of injection-molded PP containing nucleating agents was reported by a number of workers[3,12,45] and it has been suggested that enhanced polymer orientation is promoted by the presence of talc particles and is also partly due to the high rate of crystallization of these materials, which prevents melt relaxation during cooling.

The X-ray crystallinity and DSC melting enthalpy of NPP and PP produced using the same injection-molding conditions are given in Table I.

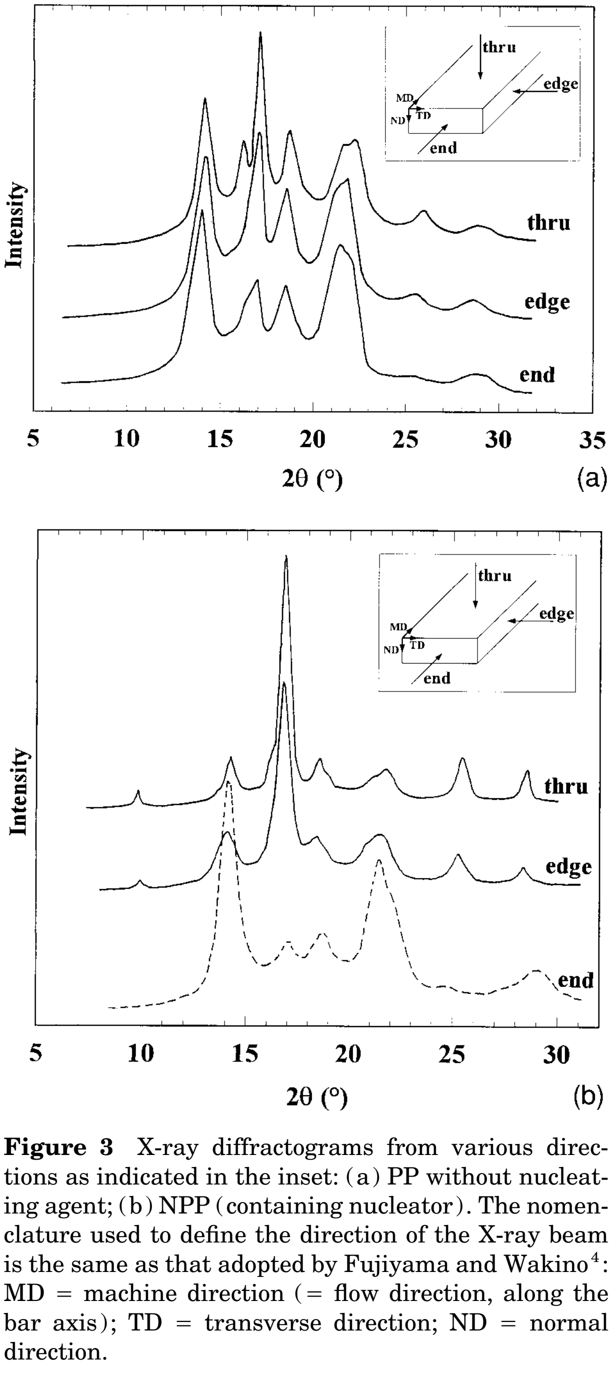

Figure 3 X-ray diffractograms from various directions as indicated in the inset: (a) PP without nucleating agent; (b) NPP (containing nucleator). The nomenclature used to define the direction of the X-ray beam is the same as that adopted by Fujiyama and Wakino[4]: MD = machine direction (= flow direction, along the bar axis); TD = transverse direction; ND = normal direction.

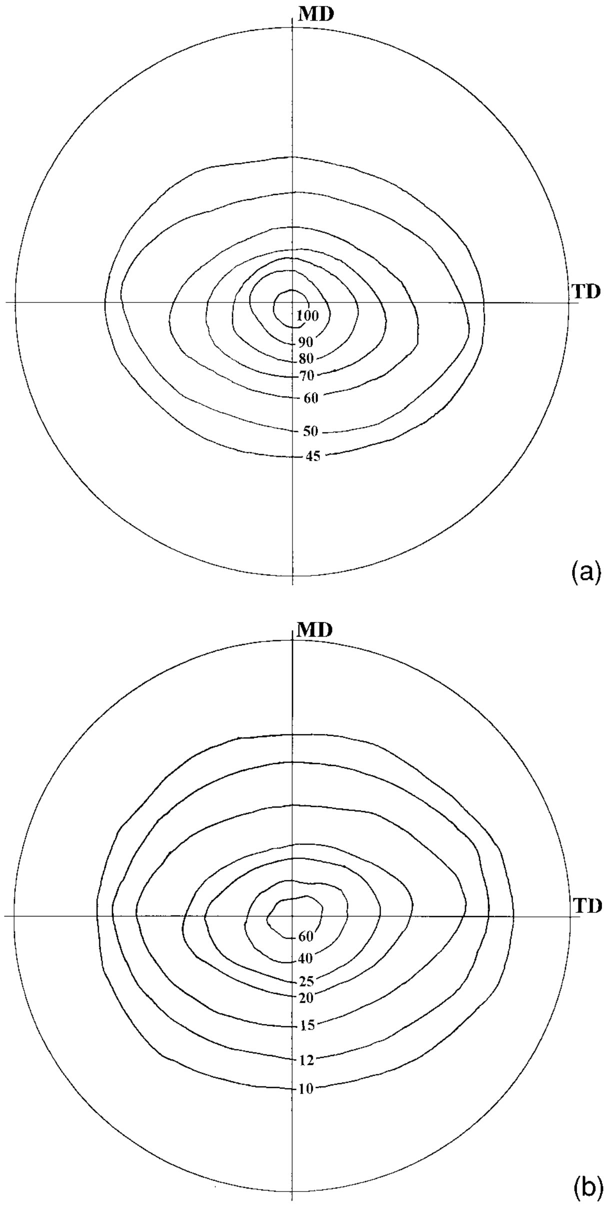

Figure 4 (040) pole figures from the surface of injection-molded bars: (a) PP (without nucleator); (b) NPP (containing nucleator).

Although the fractional crystallinity of NPP was much higher than that of PP, the values of the melting enthalpy were much more similar. This observation poses the question of which measurement technique best represents the effect of talc as a nucleator on the crystallinity of PP. For the calculation of crystallinity of NPP based on the X-ray diffractogram, the sum of the areas corresponding to the talc reflections at $2\theta = 9.4°$ and 28.7° (Fig. 2) was subtracted from the total area above the amorphous background. However, another strong reflection by the talc particles at $2\theta = 19°$ was very close to the reflections of the polymer and could not be subtracted. This may be a cause for an overestimation of the X-ray crystallinity. Another possible reason is that the shape of the amorphous background may change with orientation[46] and this is not accounted for in the method of Weidinger and Hermans[43] used in the present investigation. Table I also shows that the amount of material present as β-phase crystals (given by the B-index[47]) is much lower in NPP than in PP. This has been explained as due to preferential nucleation of the α-phase by the talc particles.[1]

The skin–core morphologies of the two samples are shown by polarized light microscopy in Figure 5. The morphology of NPP is markedly different from that of the neat PP, with a highly birefringent skin layer about 0.4 mm thick followed by another, thicker layer; then, a narrow band appears near the center of the bar, which may constitute the unoriented core. The nonnucleated material presents a much more complex structure of stratified layers and larger spherulites.

Extent of Chemical Degradation

The molecular weight and carbonyl index of the irradiated PP containing the nucleating agent are shown, respectively, in Figures 6 and 7 and compared with values for nonnucleated PP. The results for the molecular weight were indistinguishable for most exposure times investigated but the carbonyl indices of NPP were slightly lower than the ones for PP. The values for these two parameters in both materials are too close to conclude that there is a significant influence of talc on PP

Table I Crystallinity, Melting Enthalpy, and B-index of NPP and PP Obtained from the Molded Surface of Injection-Molded Bars[a]

Material	Crystallinity (%)	Melting Enthalpy (kJ/kg)	B-index
PP	46.8 ± 0.8	101.2 ± 2.1	0.16 ± 0.01
NPP	57.1 ± 1.3	102.7 ± 0.7	0.08 ± 0.01

[a] The value of melting enthalpy of NPP was corrected for the matrix concentration.

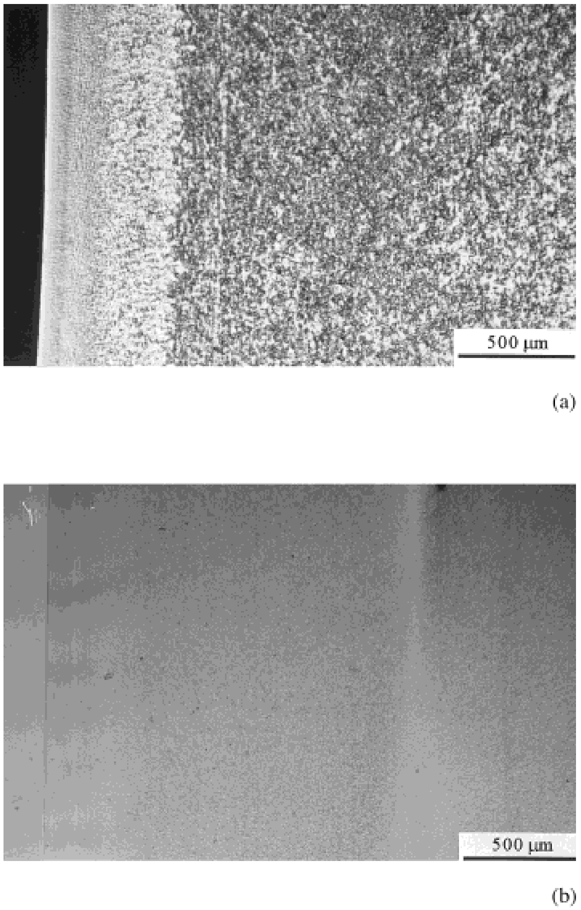

Figure 5 Polarized light microscopy of sections microtomed from (a) PP and (b) NPP.

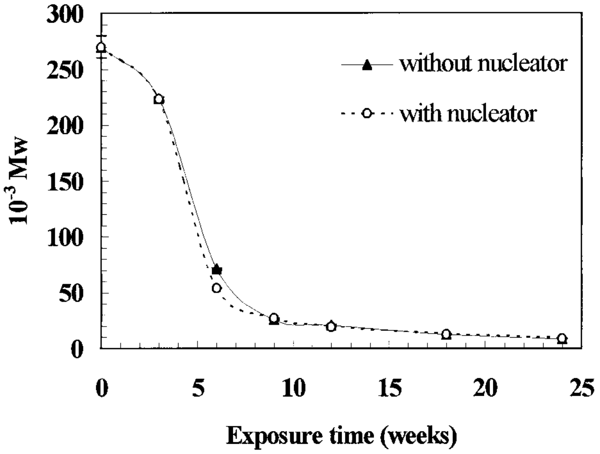

Figure 6 Effect of nucleating agent on the molecular weight of UV-irradiated PP.

photodegradation but it is worth listing some factors that could affect the rate of degradation:

(a) Talc acts as a chromophore during photodegradation. Although this possibility has not yet been confirmed (or dismissed), it is believed that it is not relevant since the use of high concentrations of talc as a filler enhanced the photostability of PP.[32]

(b) Higher molecular orientation exists in NPP than in PP: This effect would tend to reduce the photodegradability in NPP due to a lower diffusion rate of oxygen. However, the orientation was shown to have only a minor effect on the photodegradation of this grade of PP.[36]

(c) Degree of crystallinity: According to the earlier discussion, it is likely that the crystallinities of NPP and PP are similar (based on enthalpy data).

(d) The spherulite size is lower in NPP than in PP: Mucha[48] pointed out that, due to a higher permeability of oxygen in the interspherulitic than in the intraspherulitic region, the thermal stability of a PP sample with large spherulites is higher than one with small spherulites. Moreover, Nishimoto and Kagiya[49] observed that the concentration of hydroperoxide groups formed during exposure to γ-radiation decreased as the spherulite size increased. If this is also true for the photooxidation of PP, then the NPP samples would show higher rates of degradation. On the other hand, the lower the rate of crystallization, the more likely it is that chromophores are rejected by the growing spherulites to become located at their boundaries.[50] In NPP, there

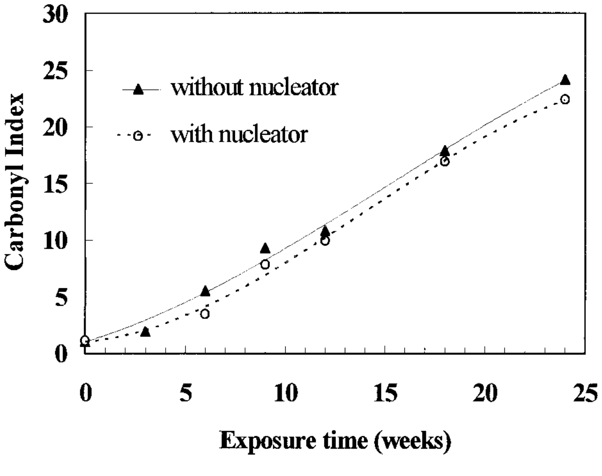

Figure 7 Effect of nucleating agent on the carbonyl index of UV-irradiated PP.

may be a lower concentration of initiating impurities at the spherulite boundaries, where the oxygen is more accessible than in the intraspherulitic region.

(e) UV absorption characteristics: The absorption characteristics of NPP and PP are nearly the same.[39]

It appears that the crystal size is the only factor that could account for differences in the rate of oxidation in these two types of samples. Since the spherulite size may affect both the diffusion of oxygen and the distribution of chromophores, with opposing consequences on the rate of degradation, the net effect was that nucleated PP and the neat polymer showed similar behavior (Figs. 6 and 7).

Mechanical Properties and Surface Fractography

Figures 8 and 9 show that a large reduction in tensile strength and maximum elongation occurred during UV exposure of both types of PP samples. This is the main practical effect of chemical degradation in ductile polymers and results from the reduction in molecular weight (Fig. 6), where the breakdown of tie chain molecules and entanglements are especially detrimental. These molecules may be more vulnerable to oxidation than the rest of the materials because they are under strain.[51] The properties of NPP samples showed the lowest value at 6 weeks exposure to ultraviolet radiation (Figs. 8 and 9). There was a sharp decrease after 3 weeks exposure and bars exposed for longer than 6 weeks showed an increase in these properties. The partial recovery in mechanical properties of PP after prolonged exposure has been attributed to the existence of a very fragile degraded layer that becomes partially detached and is unable to nucleate catastrophic failures.[38,52,53] This type of behavior has been observed in many other types of PP samples, prepared by different processing pathways[36,42] and it seems that it is a rule rather than an exception in photodegraded PP.

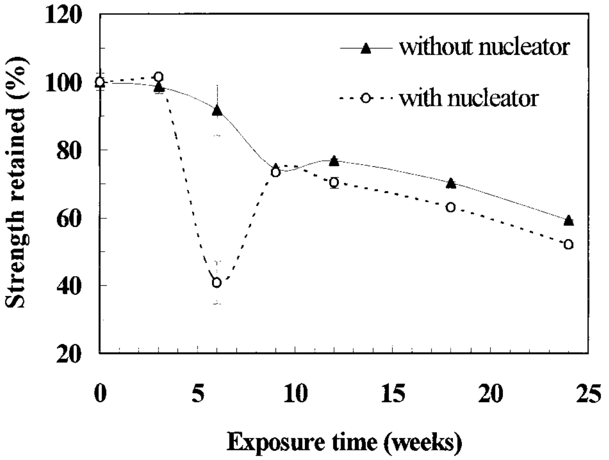

Figure 8 Tensile strength as a function of exposure time.

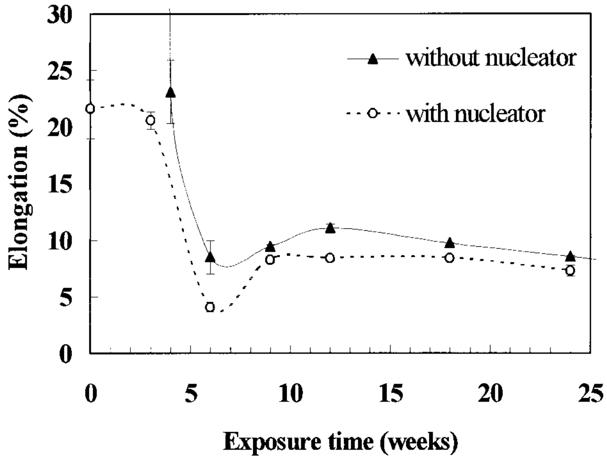

Figure 9 Maximum elongation as a function of exposure time.

Figures 8 and 9 indicate that the reduction in mechanical properties was greater in NPP than in PP for most exposure times despite the observation that the extent of chemical degradation was almost identical. It is therefore appropriate to seek a morphological explanation. Reports in the literature indicate that the tensile properties of polymers with a small spherulite size deteriorate less when chemically degraded than do those with a larger spherulite size.[36,54–56] This is opposite to the trend observed in the present work and we speculate instead that the key feature is the interspherulitic tie chain concentration. The interspherulitic boundaries are relatively weak and the interspherulitic tie molecules carry a disproportionate fraction of the load and, as a consequence, have a controlling influence on the strength.

In comparing PP and NPP, the effect of nucleant is that crystallization commences at a higher temperature and also finishes at a higher temperature in the nonisothermal conditions that prevail in injection molding. The spherulites in NPP therefore start growing at a higher temperature than those in PP, and because they impinge earlier (they have smaller size), the temperature at which they impinge is significantly higher than that at which impingement occurs in PP. The spherulite growth rate has been shown to depend on the crystallization temperature and is unaffected by the presence of nucleant.[57] Thus, the linear growth rate of the spherulites in NPP will be much smaller at the time of impingement than that in PP and this will favor a much smaller interspherulitic tie chain concentration in NPP than in PP. As a consequence, the strength advantage in the unexposed state that would be expected with the material with the smaller spherulites is opposed because the boundaries are weaker. Of even more relevance to the studies conducted here is the observation that the tie chains in the material with the smaller concentration of tie chains (NPP) will have a relatively greater importance than those in PP, so that when photodegradation causes them to break, the effect on NPP is greater than that on PP. Thus, the properties of NPP deteriorate more rapidly than those of PP on photooxidation. Our views on the effect of a nucleant on tie chain concentration are supported by measurements of swelling made by Yoshii et al. which indicated that the number of tie chain molecules was reduced in the presence of a nucleating agent.[23]

An alternative explanation to the results of Figures 8 and 9 is related to the skin–core morphology. The cracks formed on the surface of NPP during photodegradation may be able to propagate during subsequent tensile testing more easily toward the interior of the bars since NPP contains a very high orientation throughout the thickness direction. In fact, the notch sensitivity of PP increases with orientation below the surface.[58,59]

The molded surface of an NPP bar exposed for 6 weeks, then tensile tested, is displayed in Figure 10(a). The appearance is quite similar to the one of nonnucleated material exposed for the same period of time (shown elsewhere[36]), with surface cracks forming a pattern of circular arcs. The surface cracks were shown to be related to the injection flow lines generated during mold filling and they formed prior to tensile testing.[42] After 12 weeks exposure, the surface deterioration was significantly higher [Fig. 10(b)]. Very deep cracks were formed and it can be seen that the edges flaked off and some of the degraded layer had become detached from the underlying material.

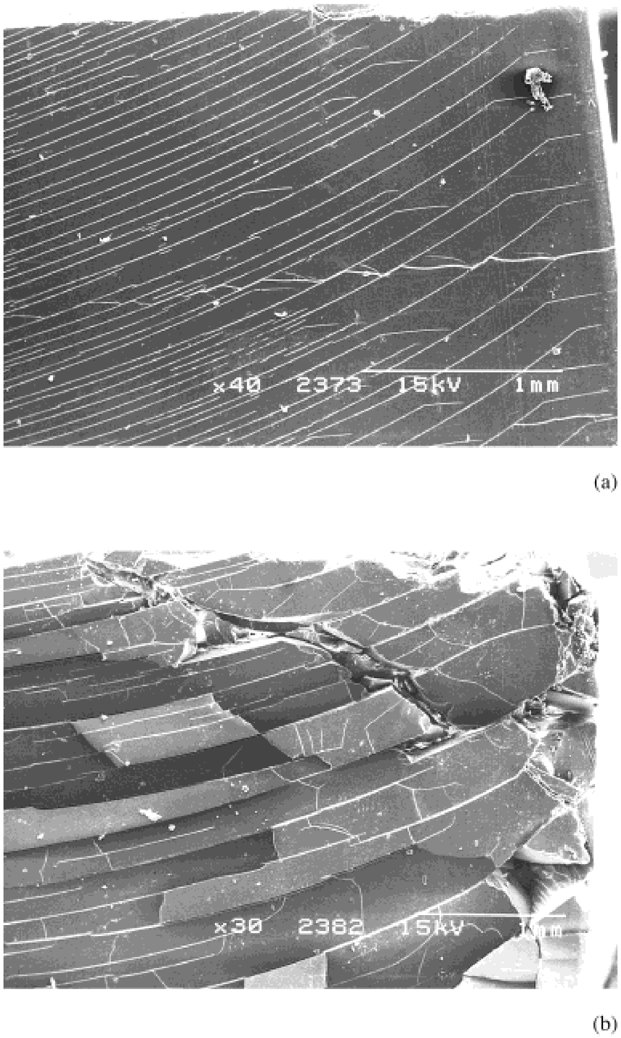

Figure 10 Exposed surfaces of NPP bars after tensile testing: (a) 6 weeks and (b) 12 weeks exposure.

The fracture surfaces of the bars shown in Figure 10 are displayed in Figure 11, showing features that are consistent with the explanation offered for the partial recovery in mechanical properties (Figs. 8 and 9). The 6 weeks exposed material [Fig. 11(a)] had a mostly smooth fracture surface showing no fibrillation, which is characteristic of brittle fracture. In this sample, the cracks formed at the molded surface propagated easily throughout the specimen thickness, leading to a catastrophic brittle failure. On the other hand, the fracture surface of a sample exposed for 12 weeks [Fig. 11(b)] showed a ductile band beneath the degraded skin which is supposed to be the reason for the partial recovery in mechanical properties.[53] During tensile testing, the cracks present in the embrittled surface layer are unable to propagate further into the sample because the degraded layer is partially detached from the remaining material. The cracks are arrested be-

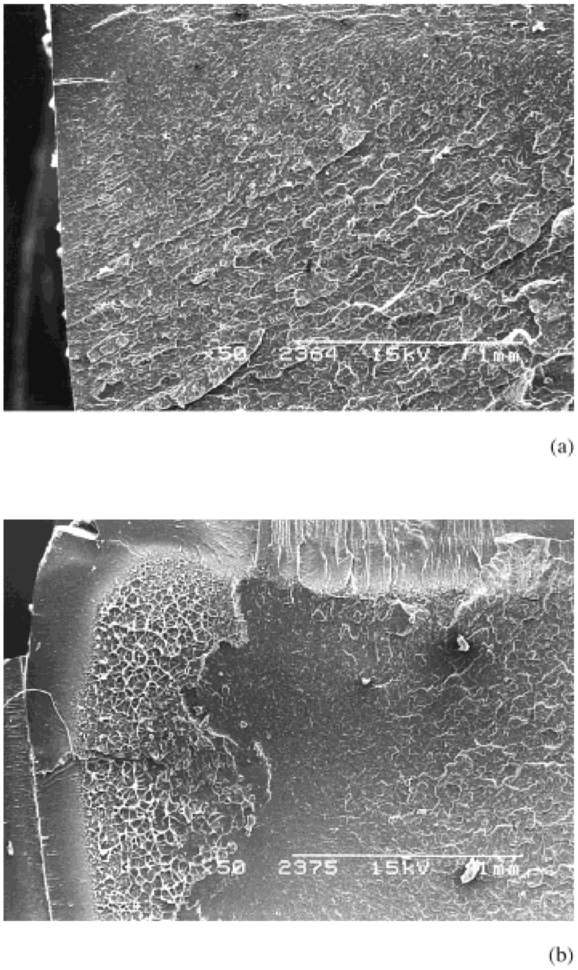

Figure 11 Fracture surfaces of the specimens shown in Figure 10 with the exposed side toward the bottom: (a) 6 weeks and (b) 12 weeks exposure.

neath the surface and reinitiation must take place from an internal site, adjacent to the ductile band. This results in toughening and better properties are recorded compared to the brittle failure for 6 weeks exposed bars [Fig. 11(a)].

Fractional Crystallinity

The X-ray crystallinity (f_c) of PP containing the nucleator is shown in Figure 12. Although the absolute values obtained may be slightly overestimated (see above), the measurements show that the evolution of f_c in NPP samples followed the same trend as in PP, with the two curves almost parallel. The increase in crystallinity during exposure is due the rearrangement of molecule segments released by chain scission in the noncrystalline region, a process called *chemicrystallization,* which is the subject of another publication.[60] Because oxygen starvation limits the amount of chain scission in the interior, the majority of chain scission events occur near the surface and the main effect of chemicrystallization is surface densification. This leads to cracks formed spontaneously at the molded surface of polymer products during UV exposure. For exposures longer than ca. 18 weeks, the molecules contained a large number of chemical irregularities like carbonyl and hydroperoxide groups, preventing further increases in fractional crystallinity[60] and a plateau value was obtained.

Differential Scanning Calorimetry

The melting thermograms of degraded PP containing the nucleating agent displayed single peaks on both first and second melting runs (the thermograms for the second run are given in Fig. 13). This contrasts with the nonnucleated polymer which showed double peaks on the second melting. It was shown elsewhere[61] that the peak duplication observed in degraded PP crystallized from the melt was due to reorganization of a phase with relatively low stability during subsequent heating in the DSC. This effect was more likely to be observed when the instability of the structure obtained from the melt was highest (as produced by fast cooling from the melt). Since the samples containing talc crystallized at much higher temperatures than did the unfilled polymer (see Fig. 16 below), a higher crystal stability is expected, preventing the reorganization of the α-phase during the DSC reheating run[62]; hence, only single

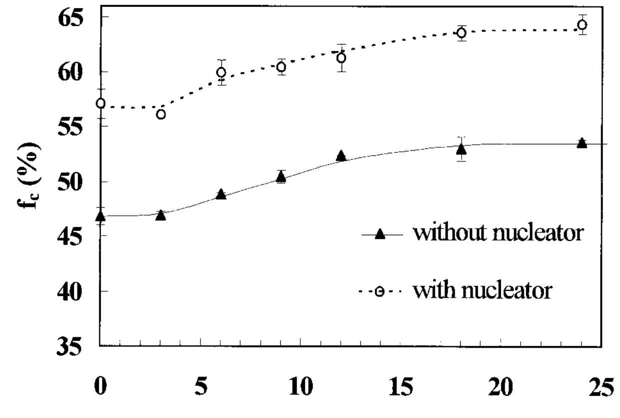

Figure 12 Effect of exposure time on the fractional crystallinity.

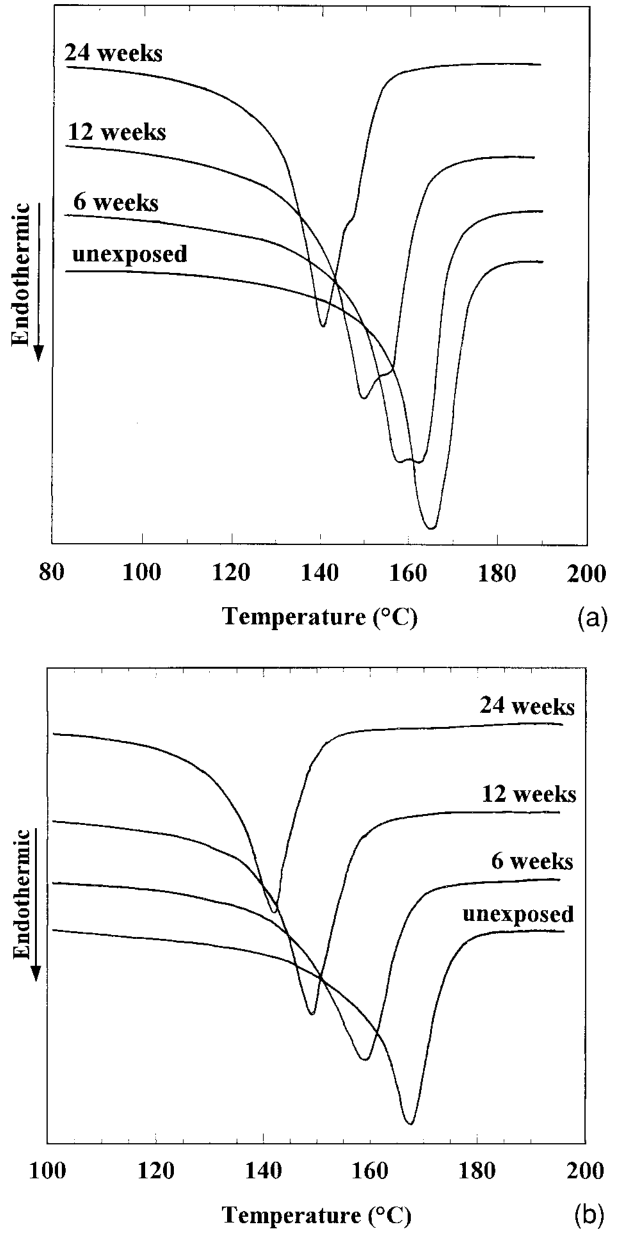

Figure 13 Melting thermograms (second run) of (a) PP and (b) NPP after various exposure times.

peaks are observed. A study of the melting behavior of photodegraded PP during the first heating run was also described elsewhere.[60]

The effect of exposure time on the melting temperatures of PP containing the nucleator is given in Figure 14. The melting temperatures of the first melting run (T_{m1}) were nearly identical to nonnucleated PP up to 12 weeks exposure, but after longer exposures, NPP displayed higher values of T_{m1}. The melting temperatures of the second run (T_{m2}) were higher for NPP samples for all exposure times. The value of T_{m2} reflects the effect of chemical defects in the molecules and may be a suitable parameter to compare the extent of degradation of similar types of samples.[36] The difference in the carbonyl index between the two types of samples (Fig. 7) may not have been large enough to account for the difference in T_{m2} shown in Figure 14(b). It is possible that the crystals in NPP are more stable since this material has a much higher recrystallization temperature (see Fig. 16), despite the fact that they contain approximately the same concentration of defects as the nonnucleated ones, as given by the carbonyl indices of Figure 7.

The melting enthalpies of weathered PP and NPP are shown in Figure 15 for the first (ΔH_{m1}) and second (ΔH_{m2}) melting runs. The general

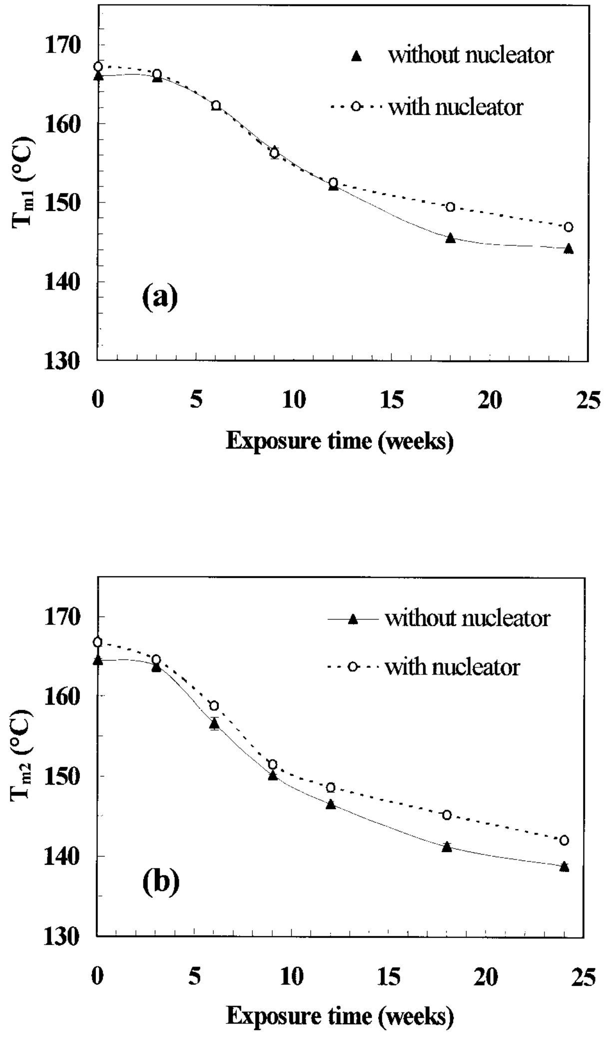

Figure 14 Effect of exposure time on the melting temperatures: (a) first melting; (b) second melting.

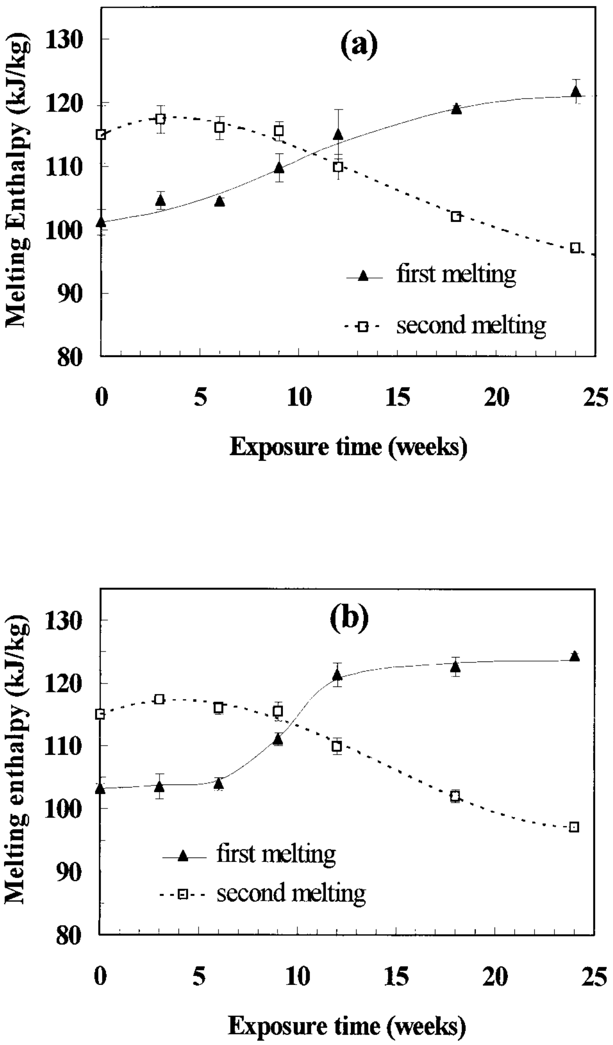

Figure 15 Effect of UV exposure on the melting enthalpies of (a) PP and (b) NPP.

trends are similar for the two types of samples. For ΔH_{m1}, there was an induction time of 6 weeks before any significant change was observed and, afterward, the enthalpy increased up to a maximum value after 18–24 weeks, which is consistent with the trend obtained by X-ray diffraction (Fig. 12). For the second heating runs, the variation of enthalpy with exposure time was also similar in the two samples with an initial increase followed by a sharp decrease after ca. 6 weeks. This is the result of a combined effect of reduction in molecule sizes and increasing concentration of chemical defects caused by chemical degradation and is discussed in more detail elsewhere.[61]

The effect of the nucleating agent on the crystallization temperature of degraded PP is shown in Figure 16. First, there is a considerable increase in the nonisothermal crystallization temperature of the unexposed PP with the addition of 0.5% talc. The increase in T_c of the polymers is generally the most important technological reason for adding nucleating agents to polymers because it leads to shorter processing cycles[9]; therefore, it is one of the main criteria to evaluate their efficiency.[15] The crystallization temperature of NPP started to decrease after 6 weeks exposure, but for all exposure times investigated, the T_c of NPP was higher than the T_c of unexposed PP. This shows that talc is a heterogeneous nucleator for PP even after extensive chemical degradation of the polymer. However, the difference in T_c between NPP and PP seems to decrease with exposure time. It is expected that, with increasing chemical defect content within the molecules, their ability to crystallize is reduced, even in the presence of heterogeneous nuclei.

CONCLUSIONS

Nucleated and nonnucleated PP showed similar rates of photodegradation but had significant differences in tensile properties, with the specimens containing a nucleating agent having poorer mechanical behavior, especially after 6 weeks exposure, when a minimum in both strength and elongation were observed. Two possible explanations for this observation have been offered: (1) It is expected that there would be a lower number of interspherulitic tie chain molecules in NPP making their scission more detrimental to the properties, and (2) the high molecular orientation in

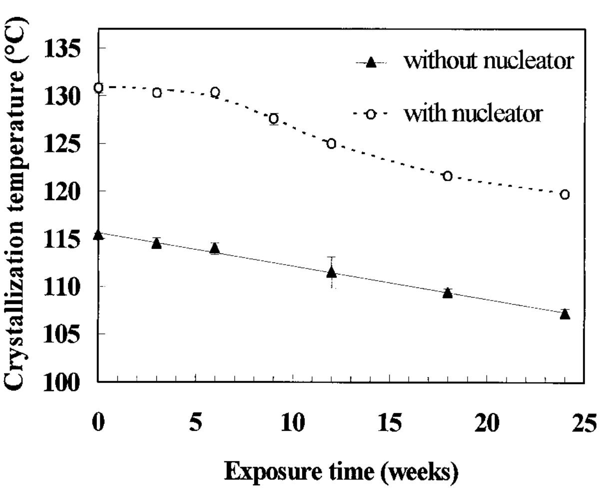

Figure 16 Crystallization temperature as a function of the exposure time for PP and NPP.

nucleated PP injection moldings makes them more sensitive to the propagation of surface cracks. The tensile strength and maximum elongation fell rapidly with exposure but then showed a partial recovery. The ability to recover mechanical properties after prolonged exposures is suggested to be due to the development of a fragile degraded layer that is unable to propagate surface cracks into the nondegraded interior, as evidenced by the fracture surface appearance. This type of behavior in PP has very important consequences in the design of components for outdoor use. If, when in service, the component is loaded at regular intervals, it will fail when the strength falls below a critical level and it will not have the chance to recover. Hence, the potential to recover may not be of much practical value even if the properties measured in the laboratory indicate that the service specifications are met after prolonged exposure if the property minimum at intermediate times is too low. Conversely, in any test program, it is essential that the interval between test exposures is small; otherwise, if there is a minimum in strength, it is likely to be missed and an overoptimistic assessment of the weatherability of the material will be obtained.

A similar increase in fractional crystallinity during photodegradation was observed for both nucleated and talc-free PP by both X-ray diffraction and DSC. The melting thermograms during the second heating run of nucleated PP showed single peaks, whereas those for nonnucleated PP displayed double peaks. In another study[61] with photodegraded PP without any nucleating agent, it was suggested that some of the PP molecules crystallize into a relatively unstable phase that transforms into a more stable phase during the DSC heating run, then melts at a higher temperature. This reorganization during heating was the reason for the double endotherm.[61] It is suggested here that the unstable phase does not form in the presence of talc as a nucleating agent, leaving only the melting endotherm of the stable phase as a single peak.

The authors are grateful to ICI for providing the materials used in this investigation and to S. R. Holding of Rapra Technology Ltd. for making the GPC measurements. M.S.R. is grateful for a CAPES scholarship funded by the Brazilian government. The equipment in the artificial weathering laboratory was funded by grants from EPSRC.

REFERENCES

1. J. Varga and F. S. Toth, *Angew. Makromol. Chem.*, **188,** 11 (1991).
2. D. Santos Filho and C. M. F. Oliveira, *Makromol. Chem.*, **194,** 279 (1993).
3. F. Rybnikar, *J. Appl. Polym. Sci.*, **38,** 1479 (1989).
4. M. Fujiyama and T. Wakino, *J. Appl. Polym. Sci.*, **42,** 9 (1991).
5. M. Huang, X. Li, and B. Fang, *J. Appl. Polym. Sci.*, **56,** 1323 (1995).
6. A. Galeski, in *Polypropylene: Structure, Blends and Composites,* J. Karger-Kocsis, Ed., Chapman & Hall, London, 1995, Vol. 1, Chap. 4, p. 116.
7. R. Gachter and H. Muller, *Plastics Additives Handbook,* Hanser, Munich, 1985.
8. C. Y. Kim and Y. C. Kim, *Polym. Eng. Sci.*, **33,** 1445 (1993).
9. F. L. Binsbergen, *Polymer,* **11,** 253 (1970).
10. F. Rybnikar, *J. Appl. Polym. Sci.*, **27,** 1479 (1982).
11. J. Menczel and J. Varga, *J. Therm. Anal.*, **28,** 161 (1983).
12. M. Fujiyama and T. Wakino, *J. Appl. Polym. Sci.*, **42,** 2739 (1991).
13. R. Zhang, H. Zheng, X. Lou, and D. Ma, *J. Appl. Polym. Sci.*, **51,** 51 (1994).
14. P. M. McGenity, J. J. Hooper, C. D. Paynter, A. M. Riley, C. Nutbeem, N. J. Elton, and J. M. Adams, *Polymer,* **33,** 5215 (1992).
15. B. Fillon, B. Lotz, A. Thierry, and J. C. Wittmann, *J. Polym. Sci. Polym. Phys. Ed.*, **31,** 1395 (1993).
16. J. I. Velasco, J. A. Desaja, and A. B. Martinez, *J. Appl. Polym. Sci.*, **61,** 125 (1996).
17. T. Kowalewski and A. Galeski, *J. Appl. Polym. Sci.*, **32,** 2919 (1986).
18. F. Rybnikar, *J. Appl. Polym. Sci.*, **42,** 2727 (1991).
19. C. M. Liauw, G. C. Lees, S. J. Hurst, R. N. Rothon, and D. C. Dobson, *Angew. Makromol. Chem.*, **235,** 193 (1996).
20. F. L. Binsbergen, *J. Polym. Sci. Polym. Phys. Ed.*, **11,** 117 (1973).
21. Z. A. Kadir, F. Yoshii, K. Makuuchi, and I. Ishigaki, *Polymer,* **30,** 1425 (1989).
22. Z. A. Kadir, F. Yoshii, K. Makuuchi, and I. Ishigaki, *Radiat. Phys. Chem.*, **39,** 535 (1992).
23. F. Yoshii, G. Meligi, T. Sasaki, K. Makuuchi, A. M. Rabie, and S. Nishimoto, *Polym. Degrad. Stab.*, **49,** 315 (1995).
24. S. H. Aziz, Z. A. Kadir, F. Yoshii, K. Makuuchi, and I. Ishigaki, *Angew. Makromol. Chem.*, **182,** 187 (1990).
25. T. Sterzynski and M. Thomas, *J. Macromol. Sci. Phys. B,* **34,** 119 (1995).
26. I. Manaf, F. Yoshii, and K. Makuuchi, *Angew. Makromol. Chem.*, **227,** 111 (1995).
27. B. Li, J. Yu, L. Zhang, and Q. Liang, *Polym. Int.*, **39,** 295 (1996).
28. A. Blaga, *Polym. Eng. Sci.*, **12,** 53 (1972).
29. M. M. Qayyum and J. R. White, *Plast. Rubb. Proc. Appl.*, **12,** 171 (1989).
30. M. M. Qayyum and J. R. White, *Polym. Compos.*, **11,** 24 (1990).

31. B. O'Donnell and J. R. White, *Polym. Degrad. Stab.,* **44,** 211 (1994).
32. M. S. Rabello and J. R. White, *Polym. Comp.,* **17,** 691 (1996).
33. M. A. Chinelatto and J. A. M. Agnelli, *Polym. Degrad. Stab.,* **50,** 13 (1995).
34. A. Casu and J. Gardette, *Polymer,* **36,** 4005 (1995).
35. L. Ogier, M. S. Rabello, and J. R. White, *J. Mater. Sci.,* **30,** 2364 (1995).
36. M. S. Rabello and J. R. White, *Polym. Degrad. Stab.,* to appear.
37. P. Vink, in *Degradation and Stabilisation of Polyolefins,* N. S. Allen, Ed., Applied Science, London, 1983, Chap. 5, p. 213.
38. B. O'Donnell, M. M. Qayyum, Li Tong, and J. R. White, *Plast. Rubb. Compos. Proc. Appl.,* **21,** 297 (1994).
39. M. S. Rabello, PhD Thesis, University of Newcastle upon Tyne, 1996.
40. B. O'Donnell, J. R. White, and S. R. Holding, *J. Appl. Polym. Sci.,* **52,** 1607 (1994).
41. J. P. Trotignon and J. Verdu, *J. Appl. Polym. Sci.,* **34,** 1 (1987).
42. M. S. Rabello and J. R. White, *Plast. Rubb. Compos. Proc. Appl.,* **25,** 237 (1996).
43. A. Weidinger and P. H. Hermans, *Makromol. Chem.,* **50,** 98 (1961).
44. W. Ruland, *Acta Crystallogr.,* **14,** 1180 (1961).
45. Z. Chen, M. C. Finet, K. Liddell, D. P. Thompson, and J. R. White, *J. Appl. Polym. Sci.,* **46,** 1429 (1992).
46. J. M. Schurz, P. Zipper, and J. Lenz, *J. Macromol. Sci. Pure Appl. Chem. A,* **30,** 603 (1993).
47. J. P. Trotignon, J. L. Lebrun, and J. Verdu, *Plast. Rubb. Proc. Appl.,* **2,** 247 (1982).
48. M. Mucha, *Colloid Polym. Sci.,* **264,** 113 (1986).
49. S. Nishimoto and T. Kagiya, in *Handbook of Polymer Degradation,* S. H. Hamid, M. B. Amin, and A. G. Maadhah, Eds., Marcel Dekker, New York, 1992.
50. A. K. Kulshreshtha, in *Handbook of Polymer Degradation,* S. H. Hamid, M. B. Amin, and A. G. Maadhah, Eds., Marcel Dekker, New York, 1992.
51. A. A. Popov, N. N. Blinov, B. E. Krisyuk, and G. E. Zaikov, *Eur. Polym. J.,* **17,** 169 (1981).
52. E. S. Sherman, A. Ram, and S. Kenig, *Polym. Eng. Sci.,* **22,** 457 (1982).
53. G. E. Schoolenberg and H. D. F. Meijer, *Polymer,* **32,** 438 (1991).
54. J. Pabiot and J. Verdu, *Polym. Eng. Sci.,* **21,** 32 (1981).
55. T. Kagiya, S. Nishimoto, Y. Watanabe, and M. Kato, *Polym. Degrad. Stab.,* **12,** 261 (1985).
56. A. Torikai, *Angew. Makromol. Chem.,* **216,** 225 (1994).
57. C. Wang and L. M. Hwang, *J. Polym. Sci. Polym. Phys. Ed.,* **34,** 47 (1996).
58. J. P. Trotignon and J. Verdu, *J. Appl. Polym. Sci.,* **34,** 19 (1987).
59. M. W. Murphy, K. Thomas, and M. J. Bevis, *Plast. Rubb. Proc. Appl.,* **9,** 3 (1988).
60. M. S. Rabello and J. R. White, to appear.
61. M. S. Rabello and J. R. White, to appear.
62. J. Varga, in *Polypropylene: Structure, Blends and Composites,* J. Karger-Kocsis, Ed., Chapman & Hall, London, 1995, Vol. 1, Chap. 3, p. 56.